

Mesangial Cell, Glomerular and Renal Vascular Responses to Endothelin in the Rat Kidney

Elucidation of Signal Transduction Pathways

Kamal F. Badr,* John J. Murray,* Mathew D. Breyer,* K. Takahashi,* T. Inagami,† and Raymond C. Harris*

With the technical assistance of Mindy Schwartzberg* and Joan Ebert*

*Departments of Medicine and †Biochemistry, Vanderbilt University School of Medicine, Nashville, Tennessee 37232

Abstract

We investigated the actions of endothelin in anesthetized rats and cultured mesangial cells. Intravenous infusion of endothelin (10 pmol/min) decreased renal blood flow by 44% at 20 min without changing arterial pressure, which subsequently rose significantly from 124 ± 3 to 133 ± 4 mmHg over 60 min. Micropuncture during the nonhypertensive period revealed increases in afferent (65%) and efferent (82%) arteriolar resistances, thereby reducing nephron plasma flow rate. The glomerular ultrafiltration coefficient (K_f) fell from 0.097 ± 0.035 to 0.031 ± 0.011 nl/(s · mmHg) as did single nephron filtration rate (41 ± 3 to 19 ± 3 nl/min). Addition of 5 nM endothelin to mesangial cells plated on a silicone rubber substrate increased the intensity and number of tension-generated wrinkles, and caused their reappearance in forskolin prerelaxed cells. 20–30 s following exposure of fura-2 loaded mesangial cells to 10 nM endothelin, single cell intracellular calcium concentration ($[Ca]_i$) increased from a mean baseline value of 66 ± 11 (SE) to a peak of 684 ± 250 nM ($P < 0.05$) followed by a sustained elevation at 145 ± 42 nM. Anion exchange HPLC revealed rapid (15 s) and dose-dependent stimulation of inositol 1,4,5-trisphosphate (IP_3) generation following exposure of [3H]myoinositol preloaded mesangial cells to 10–100 nM endothelin. Endothelin also led to intracellular alkalization of 2'7'-bis(2-carboxy-ethyl)-5-(and-6)-carboxyfluorescein (BCECF)-loaded mesangial cells and its addition was associated with dramatic augmentation of mitogenic activity. Thus, endothelin exerts potent constrictor effects on renal arterioles which precede its systemic hypertensive action. It lowers K_f and contracts mesangial cells, likely through stimulation of IP_3 generation and elevation of $[Ca]_i$. It is a potent mesangial cell mitogen. These studies define functional responses and signal transduction pathways for endothelin in the rat kidney and propose a potential role for this peptide in the control of mesangial cell function, glomerular filtration rate, and renal vascular tone.

Address reprint requests to Dr. Badr, Division of Nephrology, Department of Medicine, Vanderbilt University School of Medicine, S-3223 Medical Center North, Nashville, TN 37232.

Received for publication 16 September 1988.

J. Clin. Invest.

© The American Society for Clinical Investigation, Inc.

0021-9738/89/01/0336/07 \$2.00

Volume 83, January 1989, 336–342

Introduction

The recent isolation and identification of a novel constrictor peptide derived from large vessel endothelial cells, endothelin, and the cloning and sequence analysis of the complementary DNA of its precursor, preproendothelin (1), has aroused interest in its potential physiologic/pathophysiologic significance. In these studies, we examined the renal and systemic vascular responses to endothelin in the anesthetized rat using micropuncture techniques, and, in the light of our *in vivo* findings, explored its cellular actions and signal transduction mechanisms in cultured rat glomerular mesangial cells.

Methods

Endothelin was obtained from Peptides International (Louisville, KY) and stored as a 0.1-mM stock solution in 0.015% Triton X-305 at 4°C.

Micropuncture studies. Experiments were performed on Inactin-anesthetized euvoletic male Munich-Wistar rats weighing 225–260 g prepared for micropuncture as described previously (2). A left femoral artery catheter was used to monitor mean systemic arterial pressure (AP)¹ and sample blood. Jugular and femoral veins were catheterized for infusion of plasma, [3H]inulin (2.4 μ Ci/min) at 1.2 ml/h, and endothelin or vehicle. An electromagnetic flow probe was placed around the left renal artery and connected to a flow meter (Carolina Medical Electronics Inc., King, NC). Micropuncture measurements were performed 45–60 min after the end of surgical preparation as follows: 2-min samples of fluid were collected from surface proximal convolutions for determination of inulin concentration. Concomitantly, arterial blood was obtained for determination of hematocrit and plasma protein and inulin concentrations. Three samples of blood were obtained from surface efferent arterioles (star vessels) for determination of efferent arteriolar protein concentration. Three samples of urine from the experimental kidney were collected for the determination of flow rate, protein and inulin concentrations, and for the calculation of whole kidney GFR. Time-averaged hydraulic pressures were measured in surface glomerular capillaries (P_{GC}), proximal tubules (P_T), and surface efferent arterioles (P_E) using a servo-null micropipette transducer system (model 5; Instrumentation for Physiology and Medicine, San Diego, CA) and 2.0 M NaCl-containing pipettes (outer tip diameters: 2–4 μ m). Colloid osmotic pressure of plasma entering and leaving glomerular capillaries (π_A and π_E), single nephron GFR (SNGFR) and filtration fraction (SNFF), glomerular capillary ultrafiltration coefficient (K_f), resistance of single afferent (R_A) and efferent

1. Abbreviations used in this paper: AP, arterial pressure; BCECF, 2'7'-bis(2-carboxy-ethyl)-5-(and-6)-carboxyfluorescein; $IP_{1(2,3)}$, inositol mono-, bis-, and trisphosphate; RBF, renal blood flow.

(R_E) arterioles, and initial glomerular capillary plasma flow (Q_A), were determined using equations described in detail elsewhere (3). The concentrations of inulin in tubule fluid, plasma and urine were determined by counting samples in a beta counter (Beckman Instruments, Fullerton, CA). Protein concentration in efferent arteriolar and femoral arterial blood plasmas were determined using a fluorometric method (4). Whole kidney and micropuncture measurements were performed during an initial baseline period and then during intravenous administration of endothelin diluted in 0.9% NaCl to deliver a dose of 100 ng/kg per min (10 pm/min) at a rate of 0.025 ml/min for 80 min ($n = 6$).

Mesangial cell culture. Rat mesangial cells were isolated and cultured as described previously (5). Cell colonies were subcultured in 60 mm culture dishes, and grown routinely in RPMI 1640, supplemented with 20% FCS, penicillin 100 U/ml, and streptomycin 100 μ g/ml. Experiments carried out on cells from passages 2 to 3.

Contractility studies. Mesangial cells were seeded upon glass coverslips coated with dimethyl polysiloxane (60,000 centistokes), using the method of Harris et al. (6) and Singhal et al. (7). Experiments were conducted at 37°C 24 h after seeding using a camera-equipped inverted Nikon microscope. Endothelin (5 nM) was added and the associated changes in substratal wrinkling patterns compared to control through serial photography. Our capacity to document cell contraction with this technique has been published recently (5).

Measurement of intracellular calcium concentration ($[Ca]_i$). Mesangial cells were plated on glass or quartz coverslips 5 d before the experiment. They were deprived of serum for 72 hours and then loaded with 5–10 μ M fura-2 for 1 h. Fluorescence was measured at 37°C using continuous rapid alternating excitation (20 ms per reading) from dual monochromators set at 340 and 380 nm, respectively (Deltascan; Photon Technology International, New Brunswick, NJ). The monochromators were coupled to an inverted microscope using a 400-nm dichroic mirror and a 100 \times lens (Nikon-fluor oil immersion). Fluorescent emission greater than 435 nm was measured by photon counting (type XXX; Hamamatsu Corp., Bridgewater, NJ). The corrected fluorescent emission intensity ratio, using 340 and 380 nm excitation with background subtraction, was monitored continuously in single cells or in clusters of two to three cells. Baseline measurements were performed during continuous perfusion with Krebs buffer (114 mM NaCl, 5 mM KCl, 24 mM NaHCO₃, 1.5 mM CaCl₂, 1.0 mM MgCl₂, 10 mM glucose, 1.0 mM Na₂HPO₄, 10 mM Hepes, 0.1% BSA, pH 7.40), which was then substituted for one containing various concentrations of endothelin. At the end of each experiment, the bath was changed to a calcium-, and magnesium-free Krebs buffer modified further by the addition of 2 mM EGTA and 5 μ M ionomycin. After a stable 340/380 ratio was achieved (minimum, R_{min}), the buffer was changed back to control bath (1.5 mM calcium) plus 5 μ M ionomycin and the ratio was again allowed to stabilize (maximum, R_{max}). Intracellular calcium concentration was calculated by: $[Ca]_i = K_d \{ (R - R_{min}) / (R_{max} - R) \} \times (380_{min} / 380_{max})$ assuming the K_d for the fura-2:Ca²⁺ complex is 224 nM at 37°C (8).

Labeling mesangial cells with [³H]inositol. Cells grown to confluence in 60 mm culture dishes (10⁶ cells/dish) were incubated in *myo*-inositol free medium (RPMI) supplemented with 10% dialyzed FCS penicillin/streptomycin (~70 U/ml), and [³H]inositol (2 μ Ci/ml) in a total incubation volume of 5 ml. Preliminary experiments revealed that incorporation of label was maximal at 48 h and stable for up to 72 h. All subsequent experiments were therefore carried out on cells preincubated with [³H]inositol for 72 h and serum deprived 48 h before experiments.

Analysis of [³H]inositol phosphate formation in mesangial cells by HPLC. The formation of inositol monophosphate (IP₁), inositol bisphosphate (IP₂), and inositol trisphosphate (IP₃) in [³H]inositol loaded mesangial cells in response to endothelin was measured as follows: plates were washed with Krebs-Ringer solution containing 118 mM NaCl, 4.6 mM KCl, 24.9 mM NaHCO₃, 1 mM KH₂PO₄, 11.1 mM glucose, 1.1 mM MgSO₄, 1.0 mM CaCl₂, 5 mM Hepes, and 0.1% BSA, pH 7.4, 37°C. Increasing concentrations of endothelin (0.1 to 100 nM)

were then added in 2 ml of warmed (37°C) Krebs-Ringer and the cells incubated with the agonist for the indicated time. In experiments in which accumulation of inositol phosphates was measured at 15 min postaddition of endothelin, LiCl (10 mM) was added to the incubation medium to prevent the breakdown of IP₁. At the desired time-point following addition of endothelin to mesangial cells, the reaction was terminated by the addition of cold 10% TCA acid (final concentration) and extracted four times with ether. The pH of the samples was adjusted to pH 7–8. Before HPLC analysis each sample was passed through a 0.45 μ M HV filter (Millipore Corp., Milford, MA) after addition of a mixture of unlabeled ATP, ADP, and AMP. Inositol phosphates were separated on a Partisil SAX 10 column (Whatman, Inc., Clifton, NJ) (0.46 \times 25 cm) with a silica precolumn (Guard-Pak, Millipore Corp.). The flow rate was 1 ml/min throughout using a linear ammonium phosphate gradient system from 0 to 0.8 M ammonium phosphate (pH 3.8) over 70 min and held for an additional 20 min. The column effluent was mixed with Tru-count scintillation fluid (1:4 ratio; IN-US Corp., Fairfield, NJ) and the radioactivity was monitored by an online radioactive detector (Flo-One beta; Radiomatic Instruments and Chemical Co., Tampa, FL). The unlabeled adenine compounds were monitored at 254 nm and the retention times of the radiolabeled standards were 5, 15, 33, and 58 min for inositol, 1-IP₁, 1,4-IP₂, and 1,4,5-IP₃ (DuPont Chemicals, Wilmington, DE), respectively. Isomers of the inositol phosphates were determined by their retention times relative to the retention times of the unlabeled adenine and labeled inositol standards (9).

Intracellular pH measurements. Measurement of intracellular pH was performed using mesangial cells grown on glass coverslips. Cells were exposed for 1 h to 5 μ M 2'-bis(2-carboxy-ethyl)-5-(and-6)-carboxyfluorescein (BCECF) in a nominally bicarbonate free medium, consisting of 140 mM NaCl, 5 mM KCl, 1.5 mM CaCl₂, 1.0 mM MgCl₂, 10 mM glucose, 10 mM Hepes, pH 7.40. Fluorescent measurements were performed using a Nikon DIAPHOT TMD inverted microscope with epifluorescence attachment and a Nikon P1 Photometer (Nikon, Inc., Garden City, NY). Signals were measured from single cells or a small number of contiguous cells. The excitation wavelength was rapidly varied between 450 and 490 nm by the use of narrow band pass filters (Ditrics Optics, Hudson, MA), and the emitted fluorescence was measured at 530 nm in the absence or presence of endothelin. Intracellular pH was then determined by comparison of the ratio of the emitted fluorescence at 490 and 450 nm excitations, as extracellular pH was varied. At the end of each experiment, cytoplasmic pH was calibrated by the method of Thomas et al. (10), in which the cells were exposed to solutions of different pH, containing 130 mM KCl in the presence of the K⁺/H⁺ ionophore, nigericin (10 μ M).

Measurement of changes in mesangial cell [³H]thymidine incorporation and mitogenic activity in response to endothelin. For studies of [³H]thymidine incorporation, mesangial cells were grown in 24 well dishes. When the cells were at or near confluence, fresh medium was added containing 0.4% FCS. After 48 h of serum deprivation, the cells were exposed to fresh medium containing 0.4% FCS with or without the indicated concentration of endothelin. As a positive control, a subset of cells were exposed to 10% FCS. After 24 h exposure to endothelin, 2 μ Ci/ml of [³H]thymidine was added to each well for 6 h. Each well was then washed four times with ice-cold PBS and 1.0 ml of Hanks' solution without calcium or magnesium. Trypsin/EGTA was then added to detach the cells. An aliquot was removed for cell counts before adding 1 ml of 20% TCA. Following a 60-min incubation at 4°C, the TCA-insoluble fraction was collected on glass fiber filters (934AH; Whatman, Inc., Clifton, NJ) using a cell fractionator and the radioactivity determined using liquid scintillation spectrometry. For determination of the effect of endothelin upon increases in cell number, mesangial cells were plated in 24-well dishes at high, but subconfluent density, in RPMI with 0.4% FCS for 8 d. Cells were then exposed to endothelin, or vehicle plus 0.4% FCS. After 24 h of growth, the cells were detached and their density determined using a Coulter counter (Coulter Electronics, Hialeah, FL).

Statistical analysis. Changes from baseline to experimental conditions were compared using the paired Student's *t* test. A change was considered significant when the *P* < 0.05. Values are means ± SEM.

Results

Physiologic and micropuncture studies. During the first 20 min of its administration, endothelin was without significant effect on AP (119 ± 2 vs. 124 ± 3 mmHg, NS) or hematocrit (Hct) (47.8 ± 0.8 vs. 48.8 ± 0.7 vol%, NS). Despite constancy of these systemic parameters, endothelin infusion resulted in marked reductions in renal blood flow (RBF) and GFR which fell from 8.4 ± 0.6 to 4.7 ± 1.0 ml/min (*P* < 0.01) and from 1.13 ± 0.08 to 0.60 ± 0.08 ml/min (*P* < 0.005), respectively. Micropuncture measurements revealed similar reductions in Q_A and SNGFR which decreased from 137 ± 11 to 90 ± 14 nl/min (*P* < 0.01) and from 41.1 ± 3.0 to 18.8 ± 3.0 nl/min (*P* < 0.0005), respectively. The fall in RBF despite constant AP indicated a rise in renal vascular resistance. R_A increased from 2.32 ± 0.20 to 3.84 ± 0.48 10^{10} dyn · s · cm⁻⁵ (*P* < 0.025), while R_E increased from 1.05 ± 0.12 to 1.95 ± 0.32 10^{10} dyn · s · cm⁻⁵ (*P* < 0.05). No significant changes were noted in P_{GC} (44 ± 1 vs. 48 ± 2 mmHg) or mean net transcapillary hydraulic pressure difference (ΔP) (33 ± 2 vs. 37 ± 2 mmHg). P_E fell from 16 ± 1 to 14 ± 1 mmHg (*P* < 0.005) as did P_T (12 ± 1 to 10 ± 1 mmHg, *P* < 0.05). Significantly, K_f fell markedly during endothelin administration from 0.097 ± 0.035 to 0.031 ± 0.011 nl/(s · mmHg) (*P* < 0.05). This reduction in K_f accounted largely for the fall in SNGFR and SNFF which decreased from 0.31 ± 0.03 to 0.22 ± 0.04 (*P* < 0.05). Of interest, and despite the marked reduction in RBF and GFR during endothelin infusion, urine flow rate increased from 32 ± 8 to 40 ± 10 μ l/min (*P* < 0.05).

After 20 min of endothelin infusion, AP increased gradually to a peak value of 133 ± 4 mmHg at 60 min (*P* < 0.05 vs. baseline), and Hct rose from a baseline value of 47.8 ± 0.8 to 50.3 ± 0.3 vol% (*P* < 0.005).

Mesangial cell contraction. Addition of endothelin (5 nM) to mesangial cells plated on a rubber silicone substrate resulted in an increase in the number and intensity of tension-generated wrinkles first noted at 1 min and maximal at 15 min, indicating mesangial cell contraction (5, 11) (Fig. 1). Endothelin also restored the appearance of substratum wrinkles following forskolin-induced cellular relaxation (not shown).

[Ca]_i. As shown in a representative tracing (Fig. 2), exposure of fura-2 loaded mesangial cells to 10 nM endothelin (*n* = 8) led to a rapid rise in [Ca]_i from a mean baseline value of 66 ± 11 to a peak of 684 ± 250 nM (*P* < 0.05) 20 to 30 s after exposure to agonist. This was followed by a rapid decline to a sustained level of 145 ± 42 nM. At concentrations of 0.1 to 1 nM, no such spike was noted; instead a slow gradual rise in [Ca]_i was noted in four experiments.

Phosphoinositide turnover. Addition of increasing concentrations of endothelin to rat mesangial cells resulted in dose dependent stimulation of IP₁, IP₂, and IP₃ synthesis by these cells. Whereas HPLC profiles from cells exposed to vehicle revealed peaks corresponding to (1 or 3)-IP₁ isomers, and none corresponding to IP₂ or IP₃, addition of 10 nM endothelin (*n* = 5) resulted in severalfold increases in these IP₁ counts at 30, 60, and 900 s, and in the appearance of peaks corresponding to 4-IP₁, as well as various IP₂ and IP₃ isomers. Fig. 3 is representative of the elution profiles obtained from control and experimental samples at 1 min, and 15 min postaddition of endothelin, while the time course and magnitudes of net increases

in phosphoinositide generation following endothelin is depicted in Fig. 4. No clear responses were obtained at 1 nM concentrations and no further increases in PI generation were noted at 100 nM endothelin.

Intracellular pH. Exposure of mesangial cells to 1.0 nM endothelin (*n* = 5) resulted in an increase in intracellular pH from a baseline value of 6.79 ± 0.10 to 7.27 ± 0.07 pH units (*P* < 0.05), which was noted as early as 1 min and was maximal within 10–15 min.

[³H]Thymidine incorporation and mitogenesis. Endothelin increased [³H]thymidine uptake in mesangial cells in a dose-dependent manner. Mean counts per minute/well values were 3644 ± 642 in vehicle-treated controls (*n* = 3, each in quadruplicates) and 6,160 ± 776, 6,769 ± 692, 8,123 ± 600, and 6,789 ± 1,161 after exposure to 0.1, 1.0, 5.0, and 10.0 nM endothelin, respectively (*P* < 0.05 at all concentrations). In parallel experiments, endothelin markedly stimulated mesangial cell mitogenic activity at 24 h after its addition. This response was also dose-dependent: cell counts (in 10⁶ cells/well) were equal to 0.95 ± 0.04 following exposure to vehicle (*n* = 8), and 1.16 ± 0.08 (*n* = 4), 1.23 ± 0.02 (*n* = 6), 1.38 ± 0.04 (*n* = 5), and 1.41 ± 0.05 (*n* = 3), after exposure to 0.1, 1.0, 5.0, and 10.0 nM endothelin, respectively. Changes from control were statistically significant at all doses.

Discussion

Yanigasawa and colleagues (1) describe endothelin as “the most potent mammalian peptide known to date” based on its potency in contracting arterial strips from pig, rat, cat, rabbit, dog, and man, as well as its hypertensive action in anesthetized rats. The present studies confirm these potent constrictor effects of endothelin, since its systemic administration in doses calculated to achieve intravascular concentrations in the subnanomolar range resulted in severe renal vasoconstriction. Of particular interest was the early onset of the renal arteriolar response as compared to that of systemic vasculature, possibly indicating a greater sensitivity of the renal bed to the vasoactive actions of this peptide. This sensitivity may be even further enhanced in spontaneously hypertensive rats, as recently reported (12). Micropuncture measurements revealed that endothelin also led to a dramatic fall in the glomerular capillary ultrafiltration coefficient, K_f , attributable to the concerted contractile action of smooth muscle-containing mesangial cells, which reduces the glomerular capillary surface area available for ultrafiltration (13). This effect, in combination with the reduced renal blood flow, severely compromised the rate of glomerular filtration during endothelin administration. As endothelin infusion was maintained beyond 20 min, AP began to increase gradually over the ensuing 60 min. During this time (data not shown) RBF continued to fall despite the progressively increasing renal perfusion pressure. The late onset and the progressive nature of the increase in AP, and its failure to stabilize at an elevated value as seen with other peptides, is consistent with the suggestions of Yanigasawa and colleagues that the binding of endothelin to its putative receptor site is relatively irreversible and difficult to “wash out,” resulting in cumulative physiologic responses upon administration of agonist in initially subthreshold doses (1).

The vascular contractile responses to endothelin are independent of α -adrenergic, histaminergic, serotonergic, and arachidonate cyclooxygenase and lipoxygenase products (1). While it is conceivable that endothelin may stimulate renin-

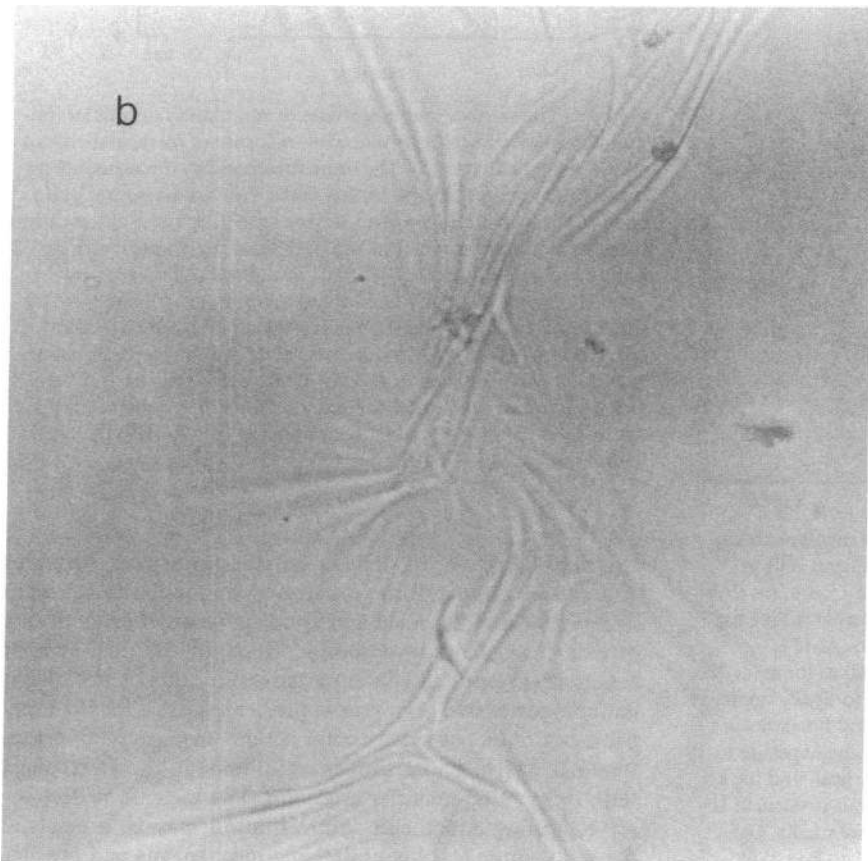
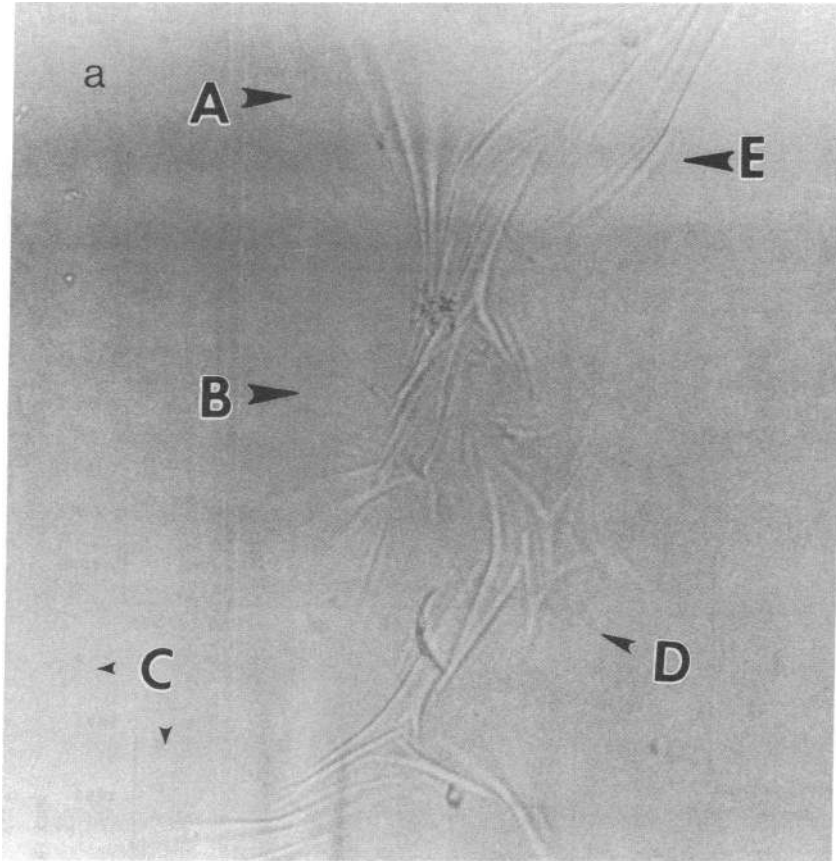


Figure 1. (a) Wrinkles generated by contractile properties of glomerular mesangial cells on silicone rubber. (b) 15 min after addition of 5 nM endothelin. Note the increase in the number of wrinkles in areas A and B, the appearance of new wrinkles in areas C and D, and the increase in the intensity of wrinkles in areas A–E. These changes were progressive and were detectable as early as one minute postaddition of endothelin. No changes were noted in vehicle-treated controls.

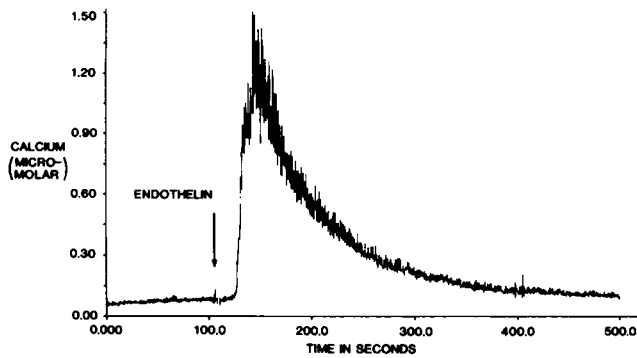


Figure 2. Representative tracing of the response of $[Ca^{2+}]_i$ to the addition of 10 nM endothelin to fura-2-loaded mesangial cells (see Methods). Note the rapid rise followed by a decline to sustained level.

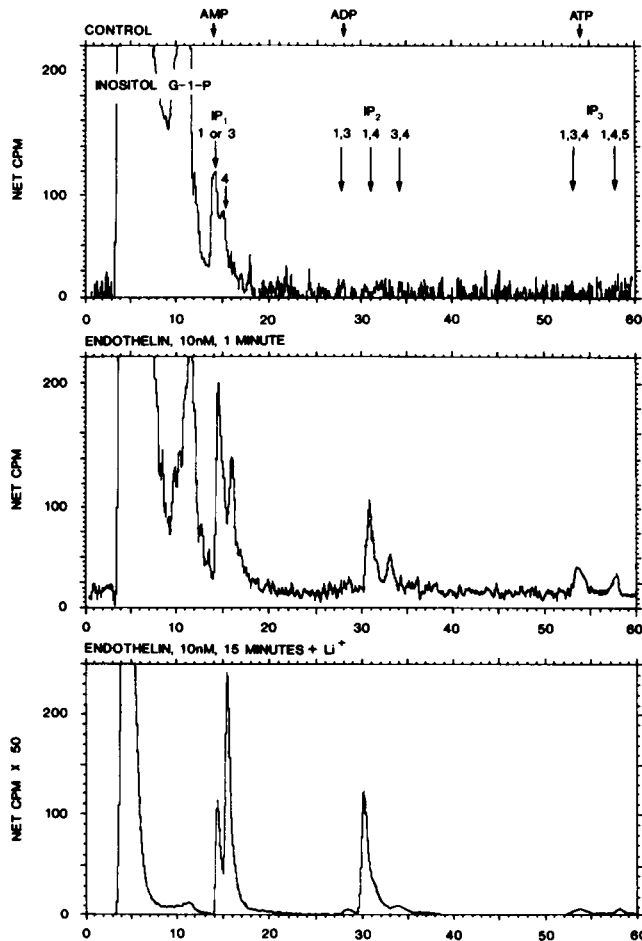


Figure 3. Representative HPLC chromatograms of cellular extracts derived from vehicle-treated control cells (*top*) and from cells exposed to endothelin (10 nM) at 1 min (*middle*) and 15 min (in the presence of Li^+ , *bottom*) postaddition of agonist. Arrows in the top panel indicate the retention times of adenine mono-(AMP), di-(ADP), and triphosphate (ATP) standards, as well as those for IP_1 , IP_2 , and IP_3 . Note that in control cells, only the 1 (or 3)- IP_1 isomer is present in significant amounts while 4- IP_1 , the major breakdown product of 1,4,5- IP_3 is a minor component. Following exposure to endothelin, there is a clear stimulation of the 4- IP_1 peak and the appearance of novel peaks corresponding to the various isomers of IP_2 and IP_3 which were not present in any of the control media. G-1-P, glycerol-1-phosphate.

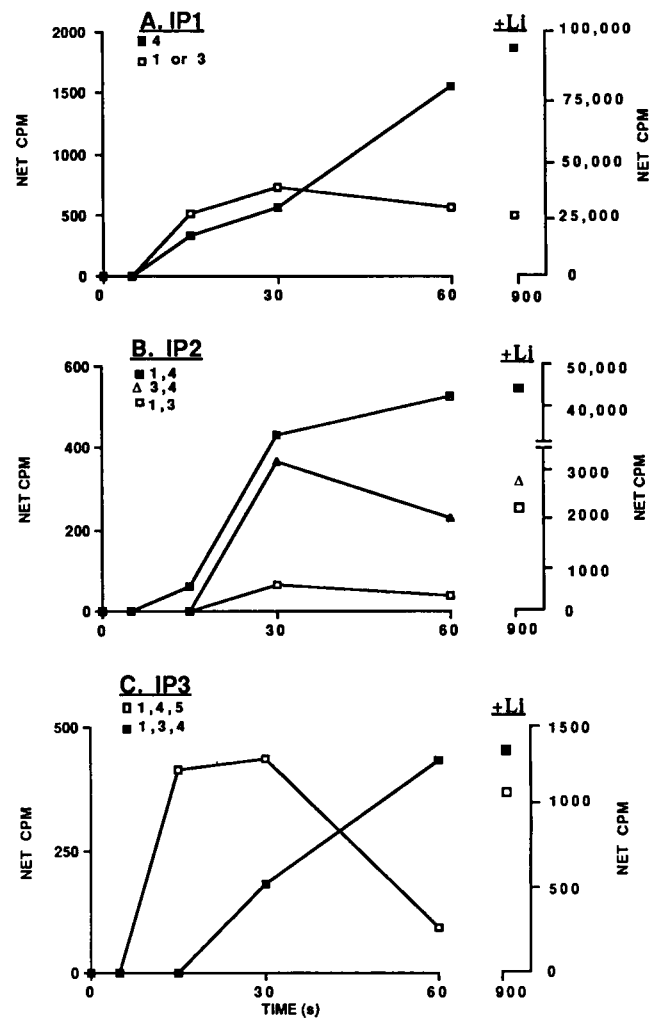


Figure 4. Time course and magnitude of stimulation of cellular inositol phosphate biosynthesis following exposure of mesangial cells to 10 nM endothelin ($n = 5$). The ordinate represents the mean net increase in counts per minute eluting under the various isomer peaks on HPLC above their respective vehicle-treated controls at the designated time points [as noted in Fig. 3, IP_2 and IP_3 isomers were absent in control samples]. (A) Stimulation of 4- IP_1 (derived from 1,4,5- IP_3) is noted as early as 15 s and increases progressively to dramatic levels (91,319 cpm) at 15 min (900 s) in the presence of Li^+ . (B) Although 1,4- IP_2 (derived from 1,4,5- IP_3) is the major product, 3,4- and 1,3- IP_2 (derived from 1,3,4- IP_3) are also formed. (C) Early (15 s) stimulation of 1,4,5- IP_3 rapidly declines in the absence of Li^+ and is followed by the gradual accumulation of 1,3,4- IP_3 , the breakdown product of 1,3,4,5- IP_4 (see text).

angiotensin release, its actions on isolated arterial strips, as well as our observations in cultured mesangial cells, argue strongly for a direct renal and systemic vascular effect of this peptide through its own specific receptors. Its dual sites of action at afferent and efferent arterioles in the absence of systemic hypertensive responses is further evidence for the independence of its renal constrictor actions from those of angiotensin II which, under similar conditions, is known to affect selectively postglomerular arterioles. The increase in Hct observed during endothelin administration may be a result of plasma volume loss; its underlying mechanisms and possible

secondary mediators remain to be investigated. Its occurrence in conjunction with the increase in urine flow seen during endothelin administration despite depressed renal hemodynamics, raises the possibility of a role for endothelin-stimulated atrial natriuretic peptide release, as has been demonstrated recently in isolated atrial myocytes (14).

Mesangial cells plated on a mobile silicone rubber substrate will induce the formation of substratal wrinkles due to the tension generated by their intrinsic actomyosin-induced contractile properties (5, 11). In the present study, endothelin increased the intensity as well as the number of these tension-generated wrinkles, indicating mesangial contraction (Fig. 1) and led to their reappearance in forskolin prerelaxed cells (not shown). These *in vitro* observations support strongly the notion that the endothelin-induced fall in K_f after its administration *in vivo* is a result of a reduction in glomerular capillary filtering surface area, secondary to mesangial cell contraction, rather than a change in the hydraulic permeability characteristics of the capillary wall.

Endothelin-induced contraction of porcine coronary artery strips is inhibited in the absence of extracellular calcium and attenuated in the presence of the calcium-channel blocker, nifedipine (1). These observations, coupled with the structural similarities between endothelin and a number of membrane-channel-acting peptide toxins, suggested that endothelin may induce its biological actions by facilitating the intracellular influx of Ca^{2+} through voltage-dependent dihydropyridine-sensitive membrane Ca^{2+} channels (1). We therefore sought to determine whether endothelin-induced mesangial cell contraction was also associated with elevations in intracellular Ca^{2+} and whether such release was linked to the intracellular generation of 1,4,5-IP₃. Two types of responses were observed: the first, occurring at endothelin concentrations of 1 nM or less, consisted of a slow progressive rise that reached a plateau within 10–20 s (not shown). The second was a classical Ca “spike” followed by a decrease to a sustained level still above control baseline typical of the Ca^{2+} signal observed following release of intracellular stores (Fig. 2). In keeping with this finding was our demonstration, using ion-exchange HPLC, that 10–100 nM endothelin induced the formation of the biologically relevant 1,4,5-isomer of IP₃ and the time-dependent metabolism of this intracellular messenger into the various phosphoinositide isomers described previously for this pathway (9), as detailed in Figs. 3 and 4.

In addition to providing insight into the biological actions of endothelin, these observations provide data regarding the heretofore undescribed metabolic fate of 1,4,5-IP₃ in mesangial cells. Although the greater proportion of 1,4,5-IP₃ appears to be a substrate for the 5-phosphatase enzyme, resulting in a major 1,4-IP₂ peak at 15 min (Fig. 4 B), it is also phosphorylated at the 3 position, a reaction catalyzed by an intracellular 3'-kinase in the presence of ATP, leading to the formation of 1,3,4,5-inositol tetrakisphosphate (IP₄). The latter is itself also a substrate for the 5-phosphatase, yielding 1,3,4-IP₃ (Fig. 4 C). Also active in mesangial cells are the 1-phosphatase [1,4-IP₂ and 1,3,4-IP₃ to 4-IP₁ (Fig. 1 A) and 3,4-IP₂ (Fig. 4 B), respectively]; the 4-phosphatase [4-IP₁ to inositol, 3,4-IP₂ to 3-IP₁ (Fig. 4 A), and 1,3,4-IP₃ to 1,3-IP₂ (Fig. 4 B)]; and finally the 3-phosphatase, which degrades 3-IP₁ to inositol and 1,3-IP₂ to 1-IP₁ (Fig. 4 A).

The temporal sequence of 1,4,5-IP₃ generation, stimulation of a Ca^{2+} transient, and cellular contraction following

exposure of rat mesangial cells to 10 nM endothelin implicates phospholipase C-mediated PIP₂ breakdown as an important signal transduction pathway for endothelin in these cells, a finding not reported to date for endothelin in other cell systems. In fact, recent communications by Hirata and others (15) fail to observe PI turnover in cultured rat vascular smooth muscle cells in response to this peptide. We find that serum deprivation for at least 72 h before the experiment, and the use of anion exchange HPLC for the analysis of the phosphoinositides clearly improve the magnitude and predictability of mesangial cell responses to endothelin. Furthermore, we fail to observe significant stimulation of PI synthesis at endothelin concentrations of 1 nM or less, and the nature of the Ca signal is also different at these concentrations. Taken together, these data raise the possibility that, at lower concentrations, endothelin may lead to increases in $[Ca^{2+}]_i$ through non-PI-mediated mechanisms, such as activation of cell membrane Ca channels (1, 15). Of interest with regard to the present studies, as well as those of Yanigasawa et al. (1) and Hirata et al. (15) is the recent report by Snyder and his colleagues (16) demonstrating that 1,3,4,5-IP₄ (formed in mesangial cells in response to endothelin—see above) induces intracellular Ca^{2+} release and 1,4,5-IP₃ stimulates extracellular Ca^{2+} influx upon microinjection into oocytes, attesting to the complexity of the regulation of $[Ca^{2+}]_i$ by inositol phosphates and the possible involvement of multiple signalling pathways in response to a common agonist.

The capacity of endothelin to induce intracellular alkalization and to act as a potent mitogen represents a novel facet of its biologic activity. Endothelin-induced alkalization is likely mediated through the activation of an amiloride-sensitive Na^+ - H^+ antiporter, as demonstrated previously in mesangial cells for other vasoconstrictors (5, 17).

In summary, the present studies describe cellular responses, signal transduction pathways, renovascular, glomerular, and systemic actions for endothelin in the rat. The cellular responses in mesangial cells include inositol phosphate turnover, elevations in intracellular calcium concentration, intracellular alkalization, mitogenesis, and contraction, suggesting the presence of endothelin-specific receptors on these cells. Taken together, these data raise the possibility of an important role for endothelin in the control of renal and systemic vascular reactivity and glomerular function during physiologic and/or pathophysiologic conditions.

Acknowledgments

This work was supported by National Institutes of Health grants DK-38667, DK-39261, HL-14192, HL-35323, DK-26657 and Veterans Administration Research Funds. Dr. Breyer is an Associate Investigator and Dr. Harris is a Research Associate in the Career Development Program of the Veterans Administration. Dr. Murray is an RJR Nabisco Scholar.

References

1. Yanigasawa, M., H. Kurihara, S. Kimura, Y. Tomobe, M. Kobayashi, Y. Mitsui, K. Goto, and T. Masaki. 1988. A novel potent vasoconstrictor peptide produced by vascular endothelial cells. *Nature (Lond.)* 332:411–415.
2. Badr, K. F., B. M. Brenner, and I. Ichikawa. 1987. Effects of leukotriene D₄ on glomerular dynamics in the rat. *Am. J. Physiol.* 22:F239–F243.

3. Deen, W. M., J. L. Troy, C. R. Robertson, and B. M. Brenner. 1973. Dynamics of glomerular ultrafiltration in the rat. IV. Determination of the ultrafiltration coefficient. *J. Clin. Invest.* 52:1500-1508.
4. Viets, J. W., W. M. Deen, J. L. Troy, and B. M. Brenner. 1978. Determination of serum protein concentration in nanoliter blood samples using fluorescamine or o-phthalaldehyde. *Anal. Biochem.* 88:513-521.
5. Harris, R. C., R. L. Hoover, H. R. Jacobson, and K. F. Badr. 1988. Evidence for glomerular actions of epidermal growth factor in the rat. *J. Clin. Invest.* 82:1028-1039.
6. Harris, A. K., P. Wild, and D. Stopak. 1980. Silicone rubber substrata: A new wrinkle in the study of cell locomotion. *Science (Wash. DC)*. 208:177-179.
7. Singhal, P. C., L. A. Scharschmidt, N. Gibbons and R. M. Hays. 1986. Contraction and relaxation of cultured mesangial cells on a silicone rubber surface. *Kidney Int.* 30:862-873.
8. Grynkiewicz, G., M. Poenie, and R. Y. Tsien. 1985. A new generation of Ca^{2+} indicators with greatly improved fluorescence properties. *J. Biol. Chem.* 260:3440-3450.
9. Dillon, S. B., J. J. Murray, M. W. Verghese, and R. Snyderman. 1987. Regulation of inositol phosphate metabolism in chemoattractant-stimulated human polymorphonuclear leukocytes. Definition of distinct dephosphorylation pathways for IP₃ isomers. *J. Biol. Chem.* 262:11546-11552.
10. Thomas, J. A., R. N. Buchsbaum, A. Zimniak, and E. Racker. 1979. Intracellular pH measurements in Ehrlich ascites cells utilizing spectroscopic probes generated in situ. *Biochemistry.* 18:2210-2215.
11. Schlondorff, D., J. A. Satriano, J. Hagege, J. Perez, and L. Baud. 1984. Effect of platelet activating factor and serum treated zymosan on PGE₂ synthesis, arachidonic acid release, and contraction of cultured rat mesangial cells. *J. Clin. Invest.* 73:1227-1231.
12. Tomobe, Y., T. Miyauchi, A. Saito, M. Yanagisawa, S. Kimura, K. Goto, and T. Masaki. 1988. Effect of endothelin on renal artery from spontaneously hypertensive and Wistar Kyoto rats. *Eur. J. Pharmacol.* 152:373-374.
13. Schlondorff, D. 1987. The glomerular mesangial cell: an expanding role for a specialized pericyte. *FASEB (Fed. Am. Soc. Exp. Biol.) J.* 1:272-281.
14. Fukuda, Y., Y. Hirata, H. Yoshimi, T. Kojima, Y. Kobayashi, M. Yanigisawa, and T. Masaki. 1988. Endothelin is a potent secretagogue for atrial natriuretic peptide in cultured rat atrial myocytes. *Biochem. Biophys. Res. Commun.* 155:167-172.
15. Hirata, Y., H. Yoshimi, S. Takata, T. X. Watanabe, S. Kumagi, K. Nakajima, and S. Sakakibara. 1988. Cellular mechanism of action by a novel vasoconstrictor endothelin in cultured vascular smooth muscle cells. *Biochem. Biophys. Res. Commun.* 154:868-875.
16. Snyder, P. M., K.-H. Krause, and M. J. Welsh. 1988. Inositol trisphosphate isomers, but not inositol 1,3,4,5-tetrakisphosphate induce calcium influx in *Xenopus laevis* oocytes. *J. Biol. Chem.* 263:11048-11051.
17. Berk, B. C., M. S. Aronow, T. A. Brock, E. Cragoe, Jr., M. A. Gimbrone, Jr., and R. W. Alexander. 1987. Angiotensin II-stimulated Na^+/H^+ exchange in cultured vascular smooth muscle cells. Evidence for protein kinase C-dependent and -independent pathways. *J. Biol. Chem.* 262:5057-5064.